Regulation of cAMP homeostasis by the efflux protein MRP4 in cardiac myocytes

Yassine Sassi,[*,†] Aniella Abi-Gerges,[*] Jeremy Fauconnier,[‡] Nathalie Mougenot,[§] Steven Reiken,[‖] Kobra Haghighi,[¶] Evangelia G. Kranias,[¶] Andrew R. Marks,[‖] Alain Lacampagne,[‡] Stefan Engelhardt,[†] Stephane N. Hatem,[*,1] Anne-Marie Lompre,[*,1] and Jean-Sébastien Hulot[*,#,1,2]

[*]Institut National de la Santé et de la Recherche Médicale (INSERM)/Université Pierre et Marie Curie, Unité Mixte de Recherche en Santé (UMRS) 956, Paris, France; [†]Institut für Pharmakologie und Toxikologie, Technische Universität München, Munich, Germany; [‡]INSERM U1046, Université Montpellier, Montpellier, France; [§]Université Pierre et Marie Curie-Paris 6, INSERM Institut Fédératif de Recherche 14 Coeur Muscle Vaisseaux (IFR CMV), Paris, France; [‖]Department of Physiology and Cellular Biophysics, Clyde and Helen Wu Center for Molecular Cardiology, Columbia University College of Physicians and Surgeons, New York, New York, USA; [¶]Department of Pharmacology and Cell Biophysics, University of Cincinnati, College of Medicine, Cincinnati, Ohio, USA; and [#]Cardiovascular Research Center, Mount Sinai School of Medicine, New York, New York, USA

ABSTRACT **Recent studies indicate that members of the multidrug-resistance protein (*MRP*) family belonging to ATP binding cassette type C (*ABCC*) membrane proteins extrude cyclic nucleotides from various cell types. This study aimed to determine whether MRP proteins regulate cardiac cAMP homeostasis. Here, we demonstrate that MRP4 is the predominant isoform present at the plasma membrane of cardiacmyocytes and that it mediates the efflux of cAMP in these cells. MRP4-deficient mice displayed enhanced cardiac myocyte cAMP formation, contractility, and cardiac hypertrophy at 9 mo of age, an effect that was compensated transiently by increased phosphodiesterase expression at young age. These findings suggest that cAMP extrusion *via* MRP4 acts together with phosphodiesterases to control cAMP levels in cardiac myocytes.—Sassi, Y., Abi-Gerges, A., Fauconnier, J., Mougenot, N., Reiken, S., Haghighi, K., Kranias, E. G., Marks, A. R., Lacampagne, A., Engelhardt, S., Hatem, S. N., Lompre, A.-M., Hulot, J. S. Regulation of cAMP homeostasis by the efflux protein MRP4 in cardiac myocytes. *FASEB J.* 26, 1009–1017 (2012). www.fasebj.org**

Key Words: cyclic nucleotides · MRP proteins · phosphodiesterases

Abbreviations: ABCC, ATP-binding cassette type C; ANF, atrial natriuretic factor; cAMP, cyclic adenosine 3′-5′-monophosphate; EC, excitation-contraction; EPAC, exchange protein directly activated by cAMP; FRET, fluorescence resonance energy transfer; FVB, Friend virus B type; GEF, guanine exchange factor; HCN, hyperpolarization-activated cyclic nucleotide; IBMX, 3-isobutyl-1-methylxanthine; iso, isoproterenol; MRP, multidrug-resistance protein; PDE, phosphodiesterase; PKA, protein kinase A; RyR, ryanodine receptor; SR, sarcoplasmic reticulum.

Cyclic adenosine 3′-5′-monophosphate (cAMP) is a second messenger that mediates the physiological effects of G_s-coupled receptors. In the heart, sympathetic activation leads to stimulation of β-adrenergic receptors, which results in the activation of adenylylcyclases and a rapid increase in cardiac myocyte cAMP. The increase in cAMP activates protein kinase A (PKA), which phosphorylates key proteins involved in excitation-contraction (EC) coupling, such as L-type calcium (Ca^{2+}) channels, phospholamban, ryanodine receptors (RyRs), and troponin I (1). PKA-dependent increases in the inward Ca^{2+}current and Ca^{2+}release and reuptake by the sarcoplasmic reticulum (SR) result in positive inotropic and lusitropic effects. cAMP also activates hyperpolarization-activated cyclic nucleotide (HCN) channels, which regulate heart rate, and the guanine exchange factor (GEF) exchange proteins directly activated by cAMP (EPACs), which have been suggested to mediate some of the prohypertrophic effects of β-adrenergic stimulation (2–4). It is now well established that cyclic nucleotides are spatially compartmentalized to enable selective activation of cellular functions and to differentiate signals from many different receptors coupled to cyclic nucleotide signaling pathways. Compartmentalized signaling has been especially well characterized for cAMP (5, 6). To date, several underlying mechanisms have been identified, including restricted synthesis of cAMP by specific localization of adenylyl cyclases in cells (7, 8); localization of PKA in specific subcellular regions *via* A-kinase anchor-

[1] These authors contributed equally to the work.

[2] Correspondence: INSERM UMR S 956 , Faculté de Médecine Pitié-Salpêtrière, 91, Bvd de l'hôpital, 75013 Paris, France. E-mail: jean-sebastien.hulot@psl.aphp.fr

doi: 10.1096/fj.11-194027

This article includes supplemental data. Please visit *http://www.fasebj.org* to obtain this information.

ing proteins (AKAPs; ref. 9); and limiting diffusion of cAMP from its site of generation within the cell by localized degradation, primarily *via* phosphodiesterases (PDEs; ref. 10). In noncardiac cells, intracellular cyclic nucleotide levels are also regulated by an active transmembrane efflux from the cytosol (11, 12). Within the large superfamily of ATP-binding cassette type C (ABCC) transporters, two members of the subfamily of multidrug-resistance proteins (MRPs), MRP4 and MRP5 (also known as ABCC4 and ABCC5) have been shown to transport cyclic nucleotides and to be expressed in the heart (11–14). Evidence also indicates nucleotide efflux from cardiac myocytes, but the underlying mechanism remains elusive (15–17). We have recently demonstrated that MRP4 acts as an endogenous regulator of intracellular cyclic nucleotide levels in vascular smooth muscle cells and plays a role in human and rat smooth muscle cell proliferation (18, 19). However, the role of MRP4-mediated cyclic nucleotide efflux in cardiac myocytes remains unknown. The present study was undertaken to examine whether MRP proteins control cAMP homeostasis in cardiacmyocytes. We show that MRP4 is present at the plasma membrane of cardiac myocytes and that it regulates intracellular cAMP levels *in vitro* and *in vivo*. These findings reveal MRP4-mediated efflux as an important mechanism for regulation of cAMP signaling in cardiac myocytes.

MATERIALS AND METHODS

Animal models

MRP4$^{-/-}$ mice were originally generated in the John Schuetz laboratory (St. Jude Children's Research Hospital, Memphis, TN, USA; ref. 20) and repeatedly back-crossed to Friend virus B-type (FVB) mice to >99% FVB (21). Generation of HCN2-cAMPs transgenic mice has been described previously (22). HCN2-cAMPs mice were crossbred with WT or *MRP4*$^{-/-}$ mice.

Quantitative real-time PCR

Total RNA was prepared with RNeasy Mini kits (Invitrogen, Carlsbad, CA, USA), and 1 μg was reverse-transcribed using a standard protocol. Gene-specific primers were used to amplify mRNA by quantitative PCR on an Mx4000 apparatus (Stratagene, La Jolla, CA, USA) using the Qiagen SYBR Green Master Mix (Qiagen, Valencia, CA, USA). The specificity of each primer set was monitored by analyzing the dissociation curve. The sample volume was 25 μl, containing 1× SYBR Green PCR master mix, 400 nM gene-specific primers, and 5 μl template. The following primer sequences were used for real-time PCR analysis: GAPDH, sense 5′-TGGCAAAGTGGAGATTGTTG-3′ and antisense 5′-CATTATCGGCCTTGACTGTG-3′; PDE1A, sense 5′-GATTGGGTTCCATGTTGCTG-3′ and antisense 5′-ATCCACAGCTGAGAGCGAGT-3′; PDE1C, sense 5′-AAGCTGAACAAGGCACAACC-3′ and antisense 5′-CTTTGGAGTTCTTCCCACGA-3′; PDE3A, sense 5′-CTCGGCTTGCCCATAAGTC-3′ and antisense 5′-CCGCAGAGTCATAGGAGTGG-3′; PDE3B, sense 5′-AAACGATCGCCTCTTGGTCT-3′ and antisense 5′-CCCAGGGTTGCTTCTTCATC-3′; PDE4A, sense 5′-CATTGGAGGTTCCAGGATTG-3′ and antisense 5′-TCTGGCCTTTGACCTTTGAC-3′; PDE4B, sense 5′-GGATGAGAGGAGCAGGGACT-3′ and antisense 5′-TGCTGCTGAAATAGCTGTGG-3′; PDE4D, sense 5′-GGACCGGATAATGGAGGAGT-3′ and antisense 5′-TCCCAGAGTGGATGAACGA-3′; PDE5A, sense 5′-TGTAGCTCAGGCCATCAACA-3′ and antisense 5′-TACCACAGAATGCCAGGTAGG-3′; ANF, sense 5′-TTTCAAGAACCTGCTAGACCAC-3′ and antisense 5′-CCCTGCTTCCTCAGTCTGCT-3′.

Western blot analysis and immunofluorescence

For immunofluorescence, the following antibodies were used: anti-MRP4 (23), anti-MRP5 (sc-5781, 1:100; Santa Cruz Biotechnology, Inc., Santa Cruz, CA, USA;), or anti-alpha-actinin (A7811, 1:500; Sigma-Aldrich, St. Louis, MO, USA) and visualized by Alexa Fluor 546 or Alexa Fluor 488 secondary antibodies (Invitrogen). Protein extraction was performed in a buffer containing protease and phosphatase inhibitors (Sigma-Aldrich), and Western blotting was performed as described previously (24). The anti-MRP4 antibody (M4I-80) was from Abcam (ab15598, 1:400; Abcam, Cambridge, MA, USA). Other antibodies included anti-calsequestrin (ABR PA-913, 1:2500; Affinity Bioreagents, Golden, CO, USA); PDE3A antibody, kindly provided by Dr. Chen Yan (University of Rochester, Rochester, NY, USA); and PDE4A5 antibody (PD4–151AP, 1:1000; Fabgennix, Frisco, TX, USA). To measure RyR phosphorylation, the following protocol was used. Mouse hearts were isotonically lysed in 2.0 ml of a buffer containing 50 mM Tris-HCl (pH 7.4), 150 mM NaCl, 20 mM NaF, 1.0 mM Na_3VO_4, and protease and phosphatase inhibitors (Roche Applied Science, Indianapolis, IN, USA). An anti-RyR antibody (4 μg 5029 Ab) was used to immunoprecipitate RyR2 from 500 μg of heart homogenate. These samples were incubated with antibody in 0.5 ml of a modified RIPA buffer (50 mM Tris-HCl, pH 7.4; 0.9% NaCl; 5.0 mM NaF; 1.0 mM Na3VO4; 1% Triton- X100, and protease inhibitors) for 1 h at 4°C. The immune complexes were incubated with protein A Sepharose beads (Sigma) at 4°C for 1 h, and the beads were washed 3 times with buffer. Proteins were separated on 6% SDS-PAGE and transferred onto nitrocellulose membranes for 1 h at 200 mA (SemiDry transfer blot, Bio-Rad, Hercules, CA, USA). Immunoblots were developed using antibodies against total RyR2 (1:2000; Affinity Bioreagents), PKA-phosphorylated RyR (P2808, 1:5000; A.R.M. laboratory) CaMKII-phosphorylated RyR (P2814, 1:5000; A.R.M. laboratory). Immunoblots were developed using the Odyssey infrared imaging system (Li-Cor Biosystems, Lincoln, NE, USA) and infrared-labeled secondary antibodies or the ECL+ detection system (GE Healthcare, Waukesha, WI, USA).

Membrane microdomain separation

The membrane fractions were separated as described previously (25). Briefly, frozen atria were homogenized in 2 ml TNE solution (20 mM Tris, 150 mM NaCl, and 1 mM EDTA, pH 7.4) containing protease inhibitor cocktail (Roche Applied Science). The homogenate was centrifuged at 1000 *g* for 5 min at 4°C. The pellet was resuspended in extraction buffer, rehomogenized, and centrifuged again at 1000 *g* for 5 min at 4°C. This latter step was repeated 3 times to enhance protein extraction efficiency. All supernatants, corresponding to the total protein fraction, were pooled, and Triton X-100 was added to 1% final concentration. All steps were performed at 4°C; at this temperature, lipid rafts are insoluble in 1% Triton X-100. After 30 min incubation on ice, the protein concentration was determined using a Bio-Rad protein assay. Sucrose solution (80%, 2 ml) was placed in a SW41 centrifuge tube (Beckman Coulter, Fullerton, CA, USA); 2 ml of the total protein (~20 mg) was placed on the sucrose solution, and the preparation was mixed with a vortex for 30 s. Sucrose (35%,

4 ml) was gently poured onto the mixture, followed by sucrose (5%, 4 ml). The gradient was then centrifuged for 18 h at 178,300 *g* and 4°C, without braking. Fractions of 1 ml were collected from the top to the bottom of the centrifuge tube (12 fractions). Each sample fraction was sonicated, its protein concentration was measured, and the same protein quantity was loaded into each lane of 12.5% polyacrylamide-SDS gels.

Adult ventricular myocyte culture and infection

Adult rat and mouse ventricular myocytes were isolated and cultured as described previously (26, 27). The adenoviruses have been described previously (18). Adult rat ventricular myocytes were infected with Ad-shMRP4 or Ad-sh Luciferase scrambled (shScr) at a MOI of 300 for 72 h.

Measurement of intracellular $Ca^{2+}$and Ca^{2+}sparks

Ventricular myocytes were loaded for 30 min at room temperature with Fluo-4 AM (5 μM; Molecular Probes, Eugene, OR, USA). Cells were then field-stimulated at 1 Hz with a 1- to 2-ms current pulse delivered *via* 2 platinum electrodes. Changes in Fluo-4 fluorescence were recorded using an LSM510 Meta Zeiss confocal microscope (×63 water-immersion objective, NA 1.2; Carl Zeiss, Oberkochen, Germany). Measurements were performed in line-scan mode (1.5 ms/line), and scanning was performed along the long axis of the cell. An excitation wavelength of 488 nm was used, and emitted light was collected through a 505-nm long-pass filter. The laser intensity used (3–6% of the maximum) had no noticeable deleterious effect on the fluorescence signal or on cell function over the time course of the experiment. To enable comparisons between cells, the change in fluorescence (ΔF) was divided by the fluorescence detected immediately before the 0.5 Hz stimulation pulse (F_0). The SR Ca^{2+} content was assessed by measuring the amplitude of cytosolic Ca^{2+} transients induced by the rapid application of caffeine (10 mM). Cardiac myocyte contractility and Ca^{2+} transient were also measured after treatment for 5 min with 1 μM of cilostamide (Tocris Bioscience, Ellisville, MO, USA).

Measurement of cardiac parameters

Noninvasive measurements of left ventricular dimensions were evaluated under isoflurane anesthesia using echocardiography-Doppler (Vivid 7 Dimension/Vivid 7 PRO; GE Medical Systems) with a probe emitting ultrasound at 9–14 MHz. The 2-dimensionally guided time-motion mode recording of the left ventricle provided the following measurements: diastolic and systolic septum and posterior wall thicknesses, internal end-diastolic and end-systolic diameters, ejection fraction, and fractional shortening of left ventricular diameter. Each set of measurements was obtained from the same cardiac cycle. At least 3 sets of measurements were obtained from 3 cardiac cycles. The Doppler measurements evaluated mitral and aortic Doppler. ECG measurements were performed in wild-type (WT) and knockout male mice at 3 mo of age. Three-lead ECGs were recorded with 25-gauge subcutaneous electrodes on a computer using an analog-digital converter (IOX 2.4.2.6; EMKA Technologies, Falls Church, VA, USA) for monitoring and later analysis. Recordings were filtered between 0.5 and 250 Hz, and a stable signal was reliably obtained before proceeding. See Supplemental Data for more details.

cAMP assay

cAMP was measured in culture supernatants and lysates of isolated adult rat ventricular myocytes by specific competitive enzyme immunoassay (cAMP [^{3}H] Assay system; GE Healthcare) as recommended by the manufacturer. Myocytes were infected for 3 d with Ad-shMRP4 or Ad-shScr. cAMP was also measured in cardiac myocytes after treatment with forskolin (10 μM, 1 h; Sigma Aldrich). Samples (200 μl) were added to 10 ml of scintillation fluid and counted on a scintillation counter. After construction of a standard curve, cAMP levels (pmol/pg protein) were determined directly.

Fluorescence resonance energy transfer (FRET) measurement

After cardiac myocyte isolation and calcium adaptation, the cells were seeded on laminin-coated coverslips. Glass coverslips with adherent cells were transferred to the experimental chamber in buffer A (137 mM NaCl, 5.4 mM KCl, 2 mM $CaCl_2$, 1 mM $MgCl_2$, and 10 mM HEPES, pH 7.3) and images were captured every 3 s on a Zeiss Axio Observer inverted microscope equipped with an oil-immersion ×40 objective, polychrome IV light source (Till Photonics, Planegg, Germany), and an Evolve-EM512 digital camera (Visitron Systems, Puchheim, Germany). FRET was monitored using MetaFluor software (Visitron Systems) as the emission ratio at 535 ± 20 and 480 ± 15 nm upon excitation at 436 ± 10 nm. The imaging data were analyzed by MetaMorph 7.0 (Visitron Systems) and Origin (Microcal, Amherst, MA, USA) software, corrected for spillover of CFP into the 535-nm channel, direct YFP excitation, and acceptor photobleaching to give a corrected YFP/CFP ratio. To study agonist-induced changes in FRET, cells were continuously superfused with buffer A plus isoproterenol (iso), with or without 3-isobutyl-1-methylxanthine (IBMX; Sigma).

Statistics

All quantitative data are reported as means ± SE. ECG data are expressed as means ± SD. Statistical analysis was performed with the Prism 3 software package (GraphPad, San Diego, CA, USA). One-way ANOVA was used to compare each parameter. *Post hoc t* test comparisons were performed to identify which group differences accounted for significant overall ANOVA results. Comparisons between ECG recordings were performed using Student's *t* test. Values of $P < 0.05$ were considered significantly different.

RESULTS

MRP4 regulates cAMP homeostasis in cardiac myocytes

MRP4, MRP5, and MRP8 have been reported to export cyclic nucleotides in several cell types (11–14), but MRP8 was not detected in the heart (28).Using immunofluorescence and Western blot analysis, we found MRP4 to be the predominant isoform expressed in the mammalian heart (**Fig. 1** and Supplemental Fig. S1). MRP4 is localized to the plasma membrane of both atrial and ventricular human myocytes (Fig. 1*A*). Interestingly, MRP4 appeared to be expressed in caveolin-containing fractions from rat atrial myocytes, cellular compartments previously shown to be enriched in

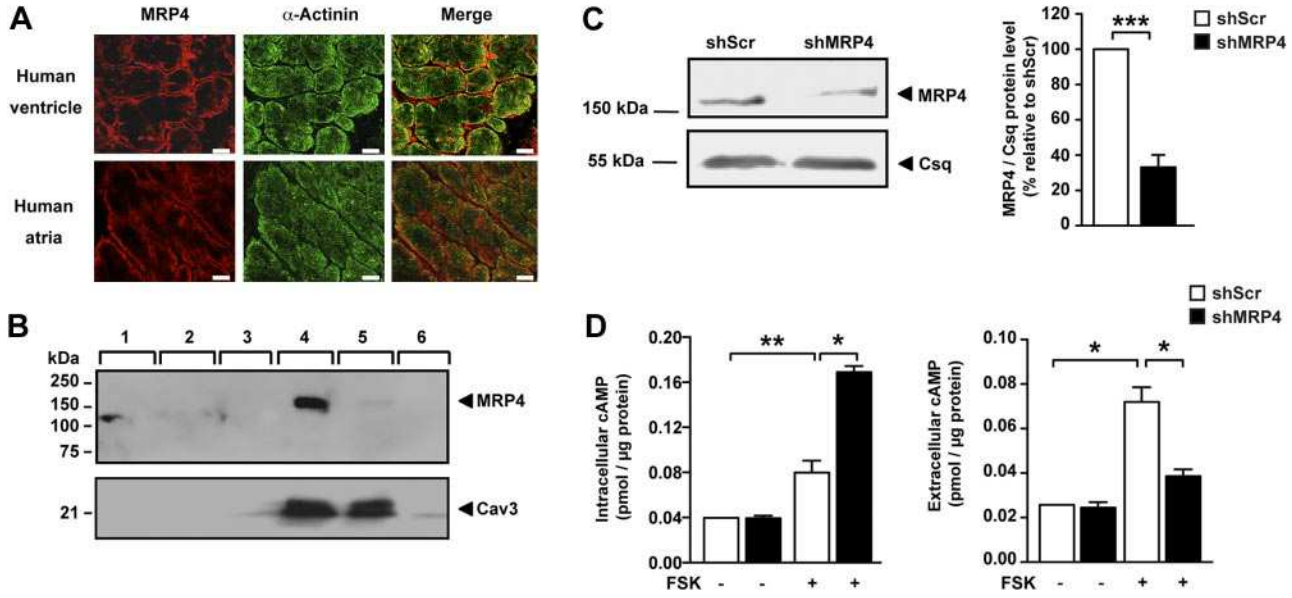

Figure 1. MRP4 expression and function in the heart. *A*) Immunodetection of MRP4 in human heart. MRP4 (red) is found on the plasma membrane of human cardiac myocytes in both atria and ventricles, whereas α-actinin (green) is present in the *Z* line. Scale bars = 10 μm. *B*) Western blot of membrane fractions from rat atrial myocytes separated on sucrose gradient. Membrane was hybridized to MRP4 antibody (top panel) and to caveolin 3 antibody (bottom panel). *C*) Representative immunoblot showing a decrease in MRP4 expression. Adult rat ventricular myocytes were infected with either Ad-shScr or Ad-shMRP4 for 3 d (n=5). *D*) Intracellular (left panel) and extracellular (right panel) cAMP levels in ventricular cardiac myocytes treated with either Ad-shScr or Ad-shMRP4 for 3 d. Cells (200,000/condition) were plated and treated with forskolin (10 μM, 1 h) or the solvent for 1 h. cAMP levels are expressed as picomoles per microgram of protein. Experiments were performed 3 times in triplicate, * $P< 0.05$; ** $P < 0.01$.

signaling molecules (Fig. 1*B*). In agreement with an earlier study, we found robust expression of MRP5 when analyzing lysates of whole ventricular myocardium (29). In contrast to MRP4, MRP5 localized to the intimal layer of vessels but not cardiac myocytes (Supplemental Fig. S1).

We initially determined the function of MRP4 in cardiac myocytes by manipulating *MRP4* expression and measuring intracellular and extracellular cAMP concentrations in transfected cells (Fig. 1*C*, *D*). MRP4 knockdown was carried out in adult rat ventricular myocytes and was achieved by adenoviral expression of a short-hairpin RNA directed against *MRP4* (Ad-shMRP4; Fig. 1*C*). An adenovirus encoding for a scrambled shRNA was used as control. Silencing *MRP4* resulted in a significant increase in intracellular cAMP levels in forskolin-stimulated (10 μM, 1 h) isolated cardiac myocytes, while it suppressed cAMP accumulation in the culture medium (Fig. 1*D*). These results indicate that MRP4 is expressed in cardiac myocytes and extrudes forskolin-induced cAMP from cardiomyocytes.

MRP4-deficient mice develop age-dependent cardiac hypertrophy

We next questioned whether MRP4 plays a role in cardiac homeostasis *in vivo* and searched for a potential cardiac phenotype of mice deficient in *MRP4* (*Mrp4*$^{-/-}$). The generation of mice with targeted disruption of the gene encoding MRP4 has been reported before (20), but cardiac function was not studied. Western blot analysis of cardiac lysates from *Mrp4*$^{-/-}$ animals confirmed a complete absence of the MRP4 protein in these animals (**Fig. 2*A***). At 3 mo of age, *Mrp4*$^{-/-}$ mice appeared to have normal cardiac morphology without significant differences in cardiac mass (Fig. 2*B*), isolated ventricular myocyte surface area (Fig. 2*C*), and echocardiographic parameters (Fig. 2*D*), as compared to WT controls. By 9 mo of age, *Mrp4*$^{-/-}$ mice developed cardiac hypertrophy, with significant increases in heart weight (Fig. 2*B*), cardiomyocyte size (Fig. 2*C*), thickness of the left ventricular wall and interventricular septum (Fig. 2*D*), and fractional shortening (Fig. 2*E*). In addition, we analyzed atrial natriuretic factor (ANF) gene expression profile in older mice. Messenger RNA expression of ANF was increased in the myocardium of aging *Mrp4*$^{-/-}$ mice (Fig. 2*F*).These data indicate a critical role for MRP4 in aging cardiac myocytes *in vivo* and prompted an assessment to determine whether cAMP homeostasis is altered in *Mrp4*$^{-/-}$ mice.

Enhanced cAMP and contractility in 9-mo-old MRP4-deficient mice

To directly determine cAMP formation in living aging cardiac myocytes from *Mrp4*$^{-/-}$mice, we used a transgenic mouse line with cardiomyocyte-specific expression of a FRET-based cAMP sensor. We had previously reported the generation of this mouse model expressing HCN2-cAMPs, a cAMP sensor that exhibits a sensitivity range optimized for the high cAMP concentrations found in adult cardiac myocytes (22). Using this mouse line, we generated double-transgenic mice deficient in *MRP4* and heterozygous for the cAMP reporter

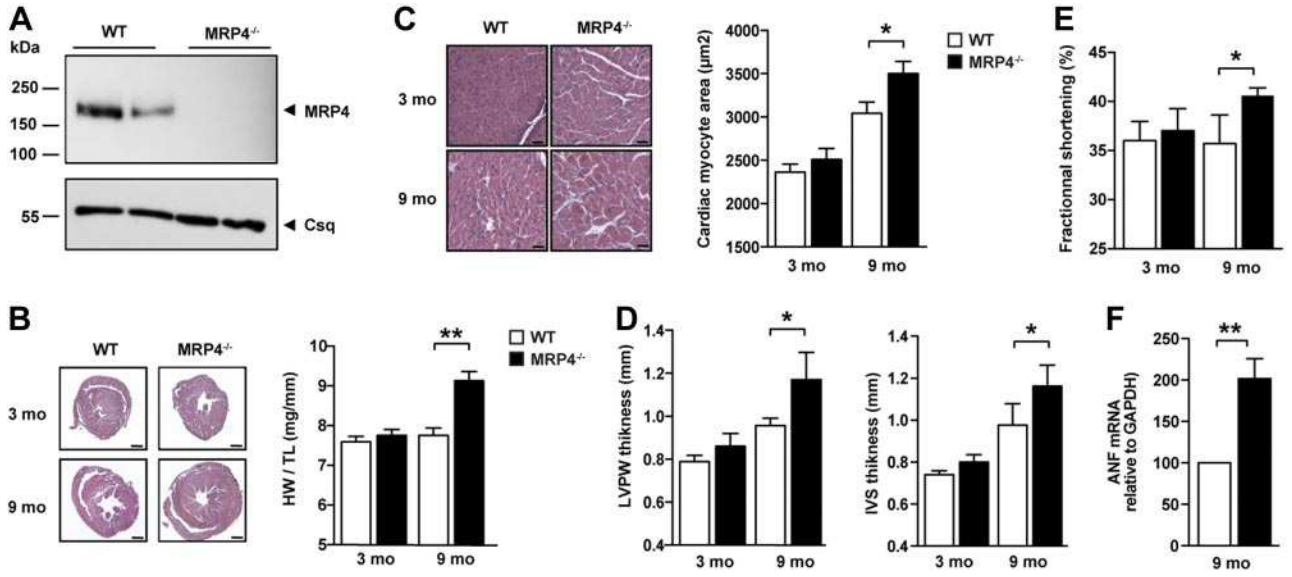

Figure 2. MRP4-deficient mice develop age-dependent cardiac hypertrophy. *A*) Western blot showing the presence of MRP4 in the heart of WT mice and its absence in *Mrp4*$^{-/-}$ mice. *B*) Histology after hematoxylin/eosin labeling and heart weight to tibia length (HW/TL) ratio of hearts from 3- and 9-mo-old *Mrp4*$^{-/-}$ and WT mice (n=6–10). *C*) Ventricular myocyte area from 3- and 9-mo-old WT and *Mrp4*$^{-/-}$ mice, showing cardiac hypertrophy in 9-mo-old *Mrp4*$^{-/-}$ mouse hearts, compared to age-matched WT (n=3–5). *D*) Echocardiography parameters showing the left ventricular posterior wall (LVPW) and interventricular septum (IVS) thickness of hearts from 3- and 9-mo-old *Mrp4*$^{-/-}$ and WT mice (n=4–6/group). *E*) Echocardiography evaluation of left ventricular fractional shortening in 9-mo-old M*rp4*$^{-/-}$ mice compared to age-matched WT (n=4–6/group). *F*) Real-time PCR analysis of ANF gene expression in the ventricular myocardium of 9-mo-old WT and *Mrp4*$^{-/-}$ mice (n=4–6). Scale bars = 1 mm (*B*); 100 µm (*C*). $^{*}P < 0.05$; $^{***}P < 0.001$.

(*Mrp4*$^{-/-}$ × myh6-HCN2-cAMPs$^{+/-}$; **Fig. 3*A***). We then analyzed camp production on a nonselective β-adrenergic stimulation in cardiac myocytes isolated from 9-mo-old WT and *Mrp4*$^{-/-}$mice. Activation of β-adrenergic receptors by iso (1 nM) induced an increase in intracellular cAMP levels that was significantly higher in cardiac myocytes isolated from 9-mo-old *Mrp4*$^{-/-}$ compared to WT mice (Fig. 3*B*, *C*). In contrast, no difference was found in 3-mo-old mice (Supplemental Fig. S2*A*). To determine whether these differences in cAMP formation would transduce into downstream signaling, we assessed cardiac myocyte cell shortening as well as Ca^{2+} transients in the presence or absence of iso. Similar to cAMP recordings, no differences were found in cell shortening (Supplemental Fig. S2*B*) or Ca^{2+} homeostasis (Supplemental Fig. S2*C*) between WT and *Mrp4*$^{-/-}$ 3-mo-old mice. In 9-mo-old animals with the absence of iso, despite an unchanged Ca^{2+} transient amplitude ($\Delta F/F_0$; Fig. 3*E*, *F*), the rate of rise ($\Delta F\,F_0^{-1}$ ms^{-1}) and rate of decay (τ) of the transient were lower in *Mrp4*$^{-/-}$ than in WT mice (Fig. 3*E*, *F*), indicating slower Ca^{2+} release and faster reuptake and/or increased extrusion by the Na-Ca exchanger. These alterations resulted in a nonsignificant decrease in SR load (5.68±0.17 in WT *vs.* 5.07±0.35 in *Mrp4*$^{-/-}$cells). Of note, 9 of 32 cells from *MRP4*$^{-/-}$ mice and 1 of 29 from WT displayed Ca^{2+} waves, which reflects the presence of delayed release after depolarization. Consistent with a slower release, the Ca^{2+} spark frequency was increased in 9-mo-old mice, whereas the amplitude $\Delta F/F_0$ was decreased (Supplemental Fig. S3*A*). Interestingly, the RyRs were hyperphosphorylated on Ser2808 (PKA site) but not on Ser2814 (Ca/calmodulin kinase site) in 9-mo-old mice (Supplemental Fig. S3*B*). However, the stimulatory effect of iso was more pronounced in *Mrp4*$^{-/-}$ than in WT mice (Fig. 3*F*).

PDEs transiently compensate for the lack of MRP4 in 3-mo-old mice

Since the 3-mo-old mice did not display any phenotype, we thought that the absence of MRP4 could be compensated by other key molecules involved in cAMP homeostasis, such as adenylyl cyclases and PDEs. Adenylyl cyclase (AC5 and AC6) expression was unchanged (data not shown), but we detected significant alterations in PDE expression. Indeed, among the 8 PDE isoforms whose expression was analyzed by quantitative real-time PCR in left ventricular myocardium from 3-mo-old animals, we found 2 (PDE3A and PDE4A) that were significantly increased in hearts from *Mrp4*$^{-/-}$ compared to WT animals (**Fig. 4*A***). This increase in gene expression was paralleled by a significant increase of PDE3A protein levels, as determined by Western blotting (Fig. 4*B*). The increase in PDE expression was transient in nature and was essentially abolished in 9-mo-old animals (Fig. 4*B*). PDE4A5 protein level was unchanged (100±10.3 *vs.* 110.4±13.3, *P*=NS in WT and *Mrp4*$^{-/-}$ mice, respectively), but we cannot exclude an alteration in expression of other PDE isoforms. To determine whether the transient increase in PDE expression was the critical factor compensating for the loss of *MRP4,* we assessed cAMP formation and downstream effects in the presence of a PDE inhibitor, IBMX (300 µM), in myocytes isolated from 3-mo-old

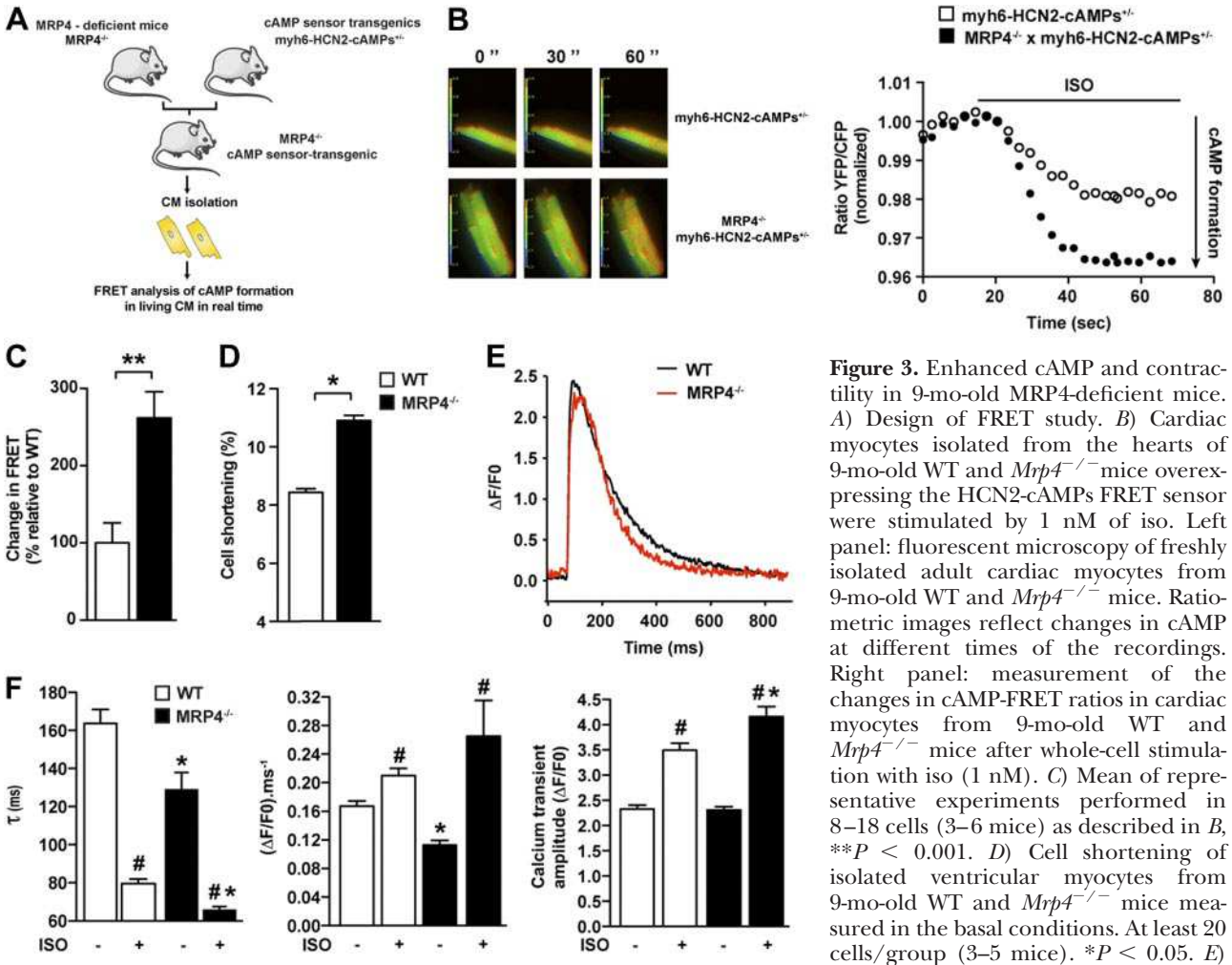

Figure 3. Enhanced cAMP and contractility in 9-mo-old MRP4-deficient mice. *A*) Design of FRET study. *B*) Cardiac myocytes isolated from the hearts of 9-mo-old WT and *Mrp4*$^{-/-}$ mice overexpressing the HCN2-cAMPs FRET sensor were stimulated by 1 nM of iso. Left panel: fluorescent microscopy of freshly isolated adult cardiac myocytes from 9-mo-old WT and *Mrp4*$^{-/-}$ mice. Ratiometric images reflect changes in cAMP at different times of the recordings. Right panel: measurement of the changes in cAMP-FRET ratios in cardiac myocytes from 9-mo-old WT and *Mrp4*$^{-/-}$ mice after whole-cell stimulation with iso (1 nM). *C*) Mean of representative experiments performed in 8–18 cells (3–6 mice) as described in *B*, $^{**}P < 0.001$. *D*) Cell shortening of isolated ventricular myocytes from 9-mo-old WT and *Mrp4*$^{-/-}$ mice measured in the basal conditions. At least 20 cells/group (3–5 mice). $^{*}P < 0.05$. *E*) Representative traces of Ca^{2+} transient of isolated ventricular myocytes from 9-mo-old WT and *Mrp4*$^{-/-}$ mice, measured in the basal condition. *F*) Ca^{2+} transient of isolated ventricular myocytes from 9-mo-old WT and *Mrp4*$^{-/-}$ mice, measured in the basal condition or in the presence of iso (100 nM): decay tau (left panel), rate of rise (middle panel), and peak Ca^{2+} transient (right panel). Experiments were performed in 30–40 cells (3–6 mice). $^{\#}P < 0.05$ *vs.* −iso; $^{*}P < 0.05$ *Mrp4*$^{-/-}$ *vs.* WT.

mice. Application of IBMX led to a significant increase in cAMP formation in sensor-transgenic cardiomyocytes isolated from *Mrp4*$^{-/-}$ as compared to control cells (Fig. 4*C*). Likewise, PDE inhibition revealed marked increase in cell shortening and modulation in Ca^{2+} cycling, as reflected by increased Ca^{2+} transient amplitude and decreased rate of rise and rate of decay (Fig. 4*D*, *E*). In addition, we examined the effects of PDE inhibition on heart rate as an alternative cAMP-regulated cardiac parameter. Again, *Mrp4*$^{-/-}$ mice (3 mo old) had similar heart rates as WT controls in the absence of a PDE inhibitor. Injection of a PDE3 inhibitor (milrinone) led to a dose-dependent increase of the heart rate that was significantly higher in *Mrp4*$^{-/-}$ compared to WT mice (Supplemental Fig. S4). Taken together, these results indicate that MRP4 acts with PDE as a key regulator of cardiac cAMP homeostasis.

DISCUSSION

Stimulation of cardiac β-adrenergic receptors by adrenaline and noradrenaline represents the major way to increase cardiac performance. Both agonists bind to and activate β1- and β2-adrenergic G_s-coupled receptors that mediate the rapid formation of the second messenger cAMP through the activation of adenylyl cyclase. This rise in intracellular cAMP determines the function of key cellular target proteins, such as cAMP-regulated channels, Ca^{2+} handling, EC coupling, and gene expression. cAMP level is delimited by intricate mechanisms of subcellular compartmentalization of its formation and degradation. The degradation is carried out through enzymatic hydrolysis by the large family of PDEs (30, 31). Our study provides evidence that extrusion of cAMP into the extracellular space represents an additional important mechanism that delimits cardiac myocyte cAMP concentrations.

Our data suggest that cAMP degradation and extrusion are tightly interconnected. Young mice deficient in *MRP4* displayed a marked up-regulation of PDE expression and activity that compensated for the impairment of cAMP extrusion, as indicated by the significant changes in cAMP formation and effects observed after PDE inhibition. Currently, we do not know the underlying mechanism that mediates enhanced transcription of PDE3 messenger

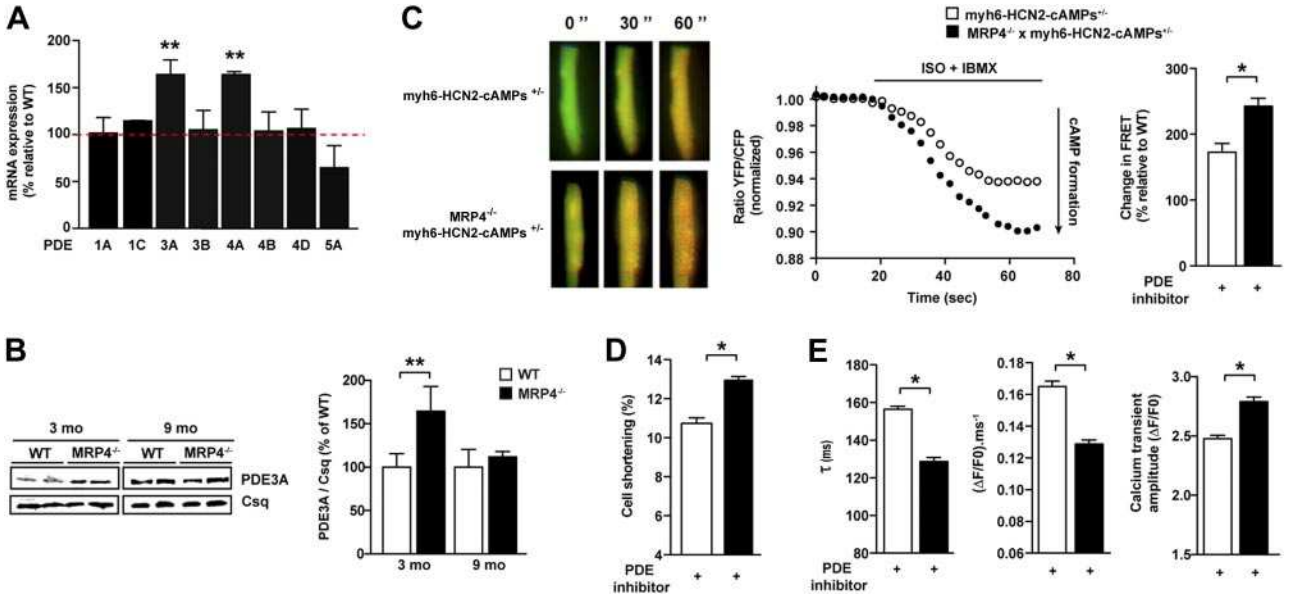

Figure 4. PDEs are up-regulated and compensate for loss of MRP4 in mice. *A*) Quantification of mRNA levels of various PDEs by real-time PCR in total cardiac extracts from 3-mo-old mice; $n = 5$/group in triplicate. *B*) Quantification of PDE3A protein by Western blot in total cardiac extracts from 3- and 9-mo-old mice (n=5). *C*) cAMP dynamics and quantification of the changes in cAMP-FRET ratios in cardiacmyocytes from 3-mo-old WT and *Mrp4*$^{-/-}$ mice after whole-cell stimulation with iso (1 nM) in combination with the nonselective PDE inhibitor IBMX (300 μM). Representative ratiometric images and experiments after iso+IBMX treatment of 7–18 cells (4–6 mice). *D, E*) Cell shortening (*D*) and Ca^{2+} transient parameters (*E*) of isolated ventricular myocytes from 3-mo-old WT and *Mrp4*$^{-/-}$ mice measured in the presence of cilostamide (1 μM; 16–24 cells, 3 mice/group). *$P < 0.05$; **$P < 0.001$.

RNA. It is tempting to speculate that cAMP leads to an activation of the PDE3 promoter, as the PDE3 promoter contains PKA consensus sites that are highly conserved (32). Similar negative feedback regulation through cyclic nucleotides has been described for other members of the PDE protein family, such as PDE4 and PDE5 (32).

Why would this compensatory mechanism that prevents the overflow of cAMP progressively disappear once a critical stage of cardiac hypertrophy has been reached (*i.e.*, ~9 mo in MRP4-deficient mice)? Previous studies have investigated changes in PDE expression and activity during cardiac hypertrophy but with contradictory observations. Several studies reported a down-regulation of PDE3 as a response to cardiac hypertrophy (33, 34), possibly mediated through the transcriptional repressor ICER (33), but others found no differences in PDE3 activity (35, 36). Because we did not observe a down-regulation of PDE3 in hypertrophic MRP4-deficient mice, we hypothesized that the hypertrophy-induced down-regulation of PDE3 previously reported by others was compensated by the transient up-regulation observed at earlier stages. Currently, we do not know whether the compensatory mechanism that prevents the overflow of cAMP progressively disappears once a critical stage of cardiac hypertrophy has been reached (*i.e.*, ~9 mo in MRP4-deficient mice) or whether the cardiac hypertrophy induces a down-regulation of the PDEs.

A recent study showed that ANF regulates the extrusion of cAMP in the pancreas through MRP4 (37). Increased ANF expression is a hallmark of cardiac hypertrophy and was observed in 9-mo-old mice. Thus, if ANF also activates MRP4 in the hypertrophic heart, the WT mice would be protected from the deleterious effect of cAMP, but this protective effect would be absent in MRP4$^{-/-}$ mice. This finding may be another reason for the decreased cardiac performance in older MRP4$^{-/-}$ mice. Interestingly, MRP4$^{-/-}$ mice are hypercontractile. The increase in cell shortening and in fractional shortening observed despite minor changes in SR Ca^{2+} load and in Ca^{2+} peak amplitude could be explained by an increase in myofilament Ca^{2+} sensitivity. EPAC could be the mediator of this effect, as shown recently (38).

Another interesting finding relates to the observation that MRP4 silencing did not affect basal cAMP concentrations but solely conditions of enhanced cAMP formation (22). This may be due to the distinct localization of MRP4. In atrial myocytes, as seen in smooth muscle cells, MRP4 is localized in caveolin-enriched membrane fractions that host signaling complexes (39). MRP4 has been reported to interact with other proteins *via* a consensus PDZ domain-binding motif at its C terminus and thereby participate in the formation of signalosomes (40). For instance, in gut cells, MRP4 interacts with the CFTR Cl^- channel *via* a MAGUK protein to regulate the concentration of cAMP at the intracellular mouth of the nucleotide gated channel (41). Further studies designed to determine the role of MRP4 in the compartmentalization of cAMP-dependent signaling in cardiac myocytes and its consequences for the regulation of cAMP targets appear warranted. However, it has been suggested that prostaglandin E2, another substrate of MRP4 (42), can induce cardiac hypertrophy by a mechanism independent of cAMP and involving the epidermal growth factor receptor transactivation (43). Even if our results

indicate significant influence of MRP4 on cAMP homeostasis, we cannot exclude that the observed changes in cardiac phenotype were also induced by additional contribution of other MRP4 endogenous substrates. This would deserve further investigations.

In addition to its important role in physiology, the cAMP signaling pathway has been identified as a major disease pathway in myocardial disease. Enhanced sympathetic activation has been found to occur in many patients with myocardial disease and to contribute to the progression of the disease. This finding is supported by data obtained from animal models where enhanced β-adrenergic signaling, *per se*, was sufficient to induce cardiac failure (44–46). Consequently, β-receptor antagonists have been tested in clinical trials and have evolved as one of the most efficient treatment options in cardiac failure (47). In contrast, interventions that enhance intracellular cAMP (such as β-agonists or pharmacological PDE inhibition) generally yielded a transient increase in cardiac performance, followed by progressive worsening of cardiac structure and function (48–50). Activators of cardiomyocyte MRP4 may represent a possible therapeutic opportunity to interfere with the detrimental consequences of the use of positive inotropic agents currently in clinical use. However, this may lead to unwanted side effects on other tissues, such as hyperproliferation of vascular smooth muscle (18, 19) and hematopoietic cells (51). This study describes a new pathway for the regulation of cAMP homeostasis in cardiac myocytes. MRP4 extrudes cAMP from cardiac myocytes and thus controls the activity of several key functional properties of the heart. FJ

The authors thank Prof. Piet Borst (NKI-Amsterdam, Amsterdam, The Netherlands) for helpful discussions and Dr. Chen Yan (University of Rochester, Rochester, NY, USA) for providing the PDE3A antibody. This work was supported by grants from the Agence Nationale de la Recherche (ANR; 09JCJC0112) and Fondation de France (2006005606) to J.S.H., by the Fondation Leducq through the CAERUS network (research agreement 05CVD03 to A.-M.L., A.R.M., and E.G.K.), and by the U.S. National Institutes of Health (grants NIH HL26057 and HL64018). Y.S. is the recipient of a Ph.D. fellowship from the French Ministère de l'Education Nationale et de la Recherche Scientifique (MENRS) and from Fondation pour la Recherche Médicale (FRM). J.S.H, S.N.H., A.-M.L. and S.E. were involved in the development of the overall study design. Y.S. planned and performed most of the experiments; A.A.G. assisted in *in vitro* experiments; J.F. performed the evaluation in isolated cardiac myocytes with the help of Y.S. and A.L.; Y.S., J.S.H., and N.M. performed the *in vivo* evaluations in mice; S.R. performed the RyR2 immunoblots. J.S.H, Y.S., S.N.H., and A.-M.L wrote the manuscript with the help of A.R.M., S.E., and A.L.; A.R.M., E.G.K., K.H., and S.N.H. assisted in conceptual aspects of the studies and interpretation of the data. All authors discussed results and contributed intellectually to the manuscript.

REFERENCES

1. Lohse, M. J., Engelhardt, S., and Eschenhagen, T. (2003) What is the role of beta-adrenergic signaling in heart failure? *Circ. Res.* **93,** 896–906
2. De Rooij, J., Zwartkruis, F. J., Verheijen, M. H., Cool, R. H., Nijman, S. M., Wittinghofer, A., and Bos, J. L. (1998) Epac is a Rap1 guanine-nucleotide-exchange factor directly activated by cyclic AMP. *Nature* **396,** 474–477
3. Metrich, M., Berthouze, M., Morel, E., Crozatier, B., Gomez, A. M., and Lezoualc'h, F. (2010) Role of the cAMP-binding protein Epac in cardiovascular physiology and pathophysiology. *Pflügers Arch.* **459,** 535–546
4. Metrich, M., Lucas, A., Gastineau, M., Samuel, J. L., Heymes, C., Morel, E., and Lezoualc'h, F. (2008) Epac mediates beta-adrenergic receptor-induced cardiomyocyte hypertrophy. *Circ. Res.* **102,** 959–965
5. Jurevicius, J., and Fischmeister, R. (1996) cAMP compartmentation is responsible for a local activation of cardiac Ca2+ channels by beta-adrenergic agonists. *Proc. Natl. Acad. Sci. U. S. A.* **93,** 295–299
6. Zaccolo, M., and Pozzan, T. (2002) Discrete microdomains with high concentration of cAMP in stimulated rat neonatal cardiac myocytes. *Science* **295,** 1711–1715
7. Ostrom, R. S., Gregorian, C., Drenan, R. M., Xiang, Y., Regan, J. W., and Insel, P. A. (2001) Receptor number and caveolar co-localization determine receptor coupling efficiency to adenylyl cyclase. *J. Biol. Chem.* **276,** 42063–42069
8. Ostrom, R. S., Gregorian, C., and Insel, P. A. (2000) Cellular release of and response to ATP as key determinants of the set-point of signal transduction pathways. *J. Biol. Chem.* **275,** 11735–11739
9. Wong, W., and Scott, J. D. (2004) AKAP signalling complexes: focal points in space and time. *Nat. Rev. Mol. Cell. Biol.* **5,** 959–970
10. Fischmeister, R., Castro, L. R., Abi-Gerges, A., Rochais, F., Jurevicius, J., Leroy, J., and Vandecasteele, G. (2006) Compartmentation of cyclic nucleotide signaling in the heart: the role of cyclic nucleotide phosphodiesterases. *Circ. Res.* **99,** 816–828
11. Borst, P., de Wolf, C., and van de Wetering, K. (2007) Multidrug resistance-associated proteins 3, 4, and 5. *Pflügers Arch.* **453,** 661–673
12. Russel, F. G., Koenderink, J. B., and Masereeuw, R. (2008) Multidrug resistance protein 4 (MRP4/ABCC4): a versatile efflux transporter for drugs and signalling molecules. *Trends Pharmacol. Sci.* **29,** 200–207
13. Ritter, C. A., Jedlitschky, G., Meyer zu Schwabedissen, H., Grube, M., Kock, K., and Kroemer, H. K. (2005) Cellular export of drugs and signaling molecules by the ATP-binding cassette transporters MRP4 (ABCC4) and MRP5 (ABCC5). *Drug Metab. Rev.* **37,** 253–278
14. Guo, Y., Kotova, E., Chen, Z. S., Lee, K., Hopper-Borge, E., Belinsky, M. G., and Kruh, G. D. (2003) MRP8, ATP-binding cassette C11 (ABCC11), is a cyclic nucleotide efflux pump and a resistance factor for fluoropyrimidines 2′,3′-dideoxycytidine and 9′-(2′-phosphonylmethoxyethyl)adenine. *J. Biol. Chem.* **278,** 29509–29514
15. Hamet, P., Pang, S. C., and Tremblay, J. (1989) Atrial natriuretic factor-induced egression of cyclic guanosine 3′:5′-monophosphate in cultured vascular smooth muscle and endothelial cells. *J. Biol. Chem.* **264,** 12364–12369
16. Kapoor, A. K., Bapat, S. K., and Saxena, V. C. (1977) Actions of glucagon on the perfused vessels of the isolated rabbit ear. *Indian J. Physiol. Pharmacol.* **21,** 133–136
17. Boixel, C., Gonzalez, W., Louedec, L., and Hatem, S. N. (2001) Mechanisms of L-type Ca(2+) current downregulation in rat atrial myocytes during heart failure. *Circ. Res.* **89,** 607–613
18. Sassi, Y., Lipskaia, L., Vandecasteele, G., Nikolaev, V. O., Hatem, S. N., Cohen Aubart, F., Russel, F. G., Mougenot, N., Vrignaud, C., Lechat, P., Lompre, A. M., and Hulot, J. S. (2008) Multidrug resistance-associated protein 4 regulates cAMP-dependent signaling pathways and controls human and rat SMC proliferation. *J. Clin. Invest.* **118,** 2747–2757
19. Hara, Y., Sassi, Y., Guibert, C., Gambaryan, N., Dorfmuller, P., Eddahibi, S., Lompre, A. M., Humbert, M., and Hulot, J. S. (2011) Inhibition of MRP4 prevents and reverses pulmonary hypertension in mice. *J. Clin. Invest.* **121,** 2888–2897
20. Leggas, M., Adachi, M., Scheffer, G. L., Sun, D., Wielinga, P., Du, G., Mercer, K. E., Zhuang, Y., Panetta, J. C., Johnston, B., Scheper, R. J., Stewart, C. F., and Schuetz, J. D. (2004) Mrp4 confers resistance to topotecan and protects the brain from chemotherapy. *Mol. Cell. Biol.* **24,** 7612–7621

21. De Wolf, C. J., Yamaguchi, H., van der Heijden, I., Wielinga, P. R., Hundscheid, S. L., Ono, N., Scheffer, G. L., de Haas, M., Schuetz, J. D., Wijnholds, J., and Borst, P. (2007) cGMP transport by vesicles from human and mouse erythrocytes. *FEBS J.* **274,** 439–450
22. Nikolaev, V. O., Bunemann, M., Schmitteckert, E., Lohse, M. J., and Engelhardt, S. (2006) Cyclic AMP imaging in adult cardiac myocytes reveals far-reaching beta1-adrenergic but locally confined beta2-adrenergic receptor-mediated signaling. *Circ. Res.* **99,** 1084–1091
23. Van Aubel, R. A., Smeets, P. H., Peters, J. G., Bindels, R. J., and Russel, F. G. (2002) The MRP4/ABCC4 gene encodes a novel apical organic anion transporter in human kidney proximal tubules: putative efflux pump for urinary cAMP and cGMP. *J. Am. Soc. Nephrol.* **13,** 595–603
24. El-Haou, S., Balse, E., Neyroud, N., Dilanian, G., Gavillet, B., Abriel, H., Coulombe, A., Jeromin, A., and Hatem, S. N. (2009) Kv4 potassium channels form a tripartite complex with the anchoring protein SAP97 and CaMKII in cardiac myocytes. *Circ. Res.* **104,** 758–769
25. Abi-Char, J., Maguy, A., Coulombe, A., Balse, E., Ratajczak, P., Samuel, J. L., Nattel, S., and Hatem, S. N. (2007) Membrane cholesterol modulates Kv1.5 potassium channel distribution and function in rat cardiomyocytes. *J. Physiol.* **582,** 1205–1217
26. Henaff, M., Antoine, S., Mercadier, J. J., Coulombe, A., and Hatem, S. N. (2002) The voltage-independent B-type Ca2+ channel modulates apoptosis of cardiac myocytes. *FASEB J.* **16,** 99–101
27. Fauconnier, J., Andersson, D. C., Zhang, S. J., Lanner, J. T., Wibom, R., Katz, A., Bruton, J. D., and Westerblad, H. (2007) Effects of palmitate on Ca(2+) handling in adult control and ob/ob cardiomyocytes: impact of mitochondrial reactive oxygen species. *Diabetes* **56,** 1136–1142
28. Bera, T. K., Lee, S., Salvatore, G., Lee, B., and Pastan, I. (2001) MRP8, a new member of ABC transporter superfamily, identified by EST database mining and gene prediction program, is highly expressed in breast cancer. *Mol. Med.* **7,** 509–516
29. Dazert, P., Meissner, K., Vogelgesang, S., Heydrich, B., Eckel, L., Bohm, M., Warzok, R., Kerb, R., Brinkmann, U., Schaeffeler, E., Schwab, M., Cascorbi, I., Jedlitschky, G., and Kroemer, H. K. (2003) Expression and localization of the multidrug resistance protein 5 (MRP5/ABCC5), a cellular export pump for cyclic nucleotides, in human heart. *Am. J. Pathol.* **163,** 1567–1577
30. Houslay, M. D., Baillie, G. S., and Maurice, D. H. (2007) cAMP-Specific phosphodiesterase-4 enzymes in the cardiovascular system: a molecular toolbox for generating compartmentalized cAMP signaling. *Circ. Res.* **100,** 950–966
31. Conti, M., and Beavo, J. (2007) Biochemistry and physiology of cyclic nucleotide phosphodiesterases: essential components in cyclic nucleotide signaling. *Annu. Rev. Biochem.* **76,** 481–511
32. Omori, K., and Kotera, J. (2007) Overview of PDEs and their regulation. *Circ. Res.* **100,** 309–327
33. Yan, C., Miller, C. L., and Abe, J. (2007) Regulation of phosphodiesterase 3 and inducible cAMP early repressor in the heart. *Circ. Res.* **100,** 489–501
34. Abi-Gerges, A., Richter, W., Lefebvre, F., Mateo, P., Varin, A., Heymes, C., Samuel, J. L., Lugnier, C., Conti, M., Fischmeister, R., and Vandecasteele, G. (2009) Decreased expression and activity of cAMP phosphodiesterases in cardiac hypertrophy and its impact on beta-adrenergic cAMP signals. *Circ. Res.* **105,** 784–792
35. Takahashi, K., Osanai, T., Nakano, T., Wakui, M., and Okumura K. (2002) Enhanced activities and gene expression of phosphodiesterase types 3 and 4 in pressure-induced congestive heart failure. *Heart Vessels* **16,** 249–256
36. Movsesian, M. A., Smith, C. J., Krall, J., Bristow, M. R., and Manganiello, V. C. (1991) Sarcoplasmic reticulum-associated cyclic adenosine 5′-monophosphate phosphodiesterase activity in normal and failing human hearts. *J. Clin. Invest.* **88,** 15–19
37. Rodriguez, M. R., Diez, F., Ventimiglia, M. S., Morales, V., Copsel, S., Vatta, M. S., Davio, C. A., and Bianciotti, L. G. (2011) Atrial natriuretic factor stimulates efflux of cAMP in rat exocrine pancreas via multidrug resistance-associated proteins. *Gastroenterology* **140,** 1292–1302
38. Cazorla, O., Lucas, A., Poirier, F., Lacampagne, A., and Lezoualc'h, F. (2009) The cAMP binding protein Epac regulates cardiac myofilament function. *Proc. Natl. Acad. Sci. U. S. A.* **106,** 14144–14149
39. Balijepalli, R. C., Foell, J. D., Hall, D. D., Hell, J. W., and Kamp, T. J. (2006) Localization of cardiac L-type Ca(2+) channels to a caveolar macromolecular signaling complex is required for beta(2)-adrenergic regulation. *Proc. Natl. Acad. Sci. U. S. A.* **103,** 7500–7505
40. Russel, F. G., Masereeuw, R., and van Aubel, R. A. (2002) Molecular aspects of renal anionic drug transport. *Annu. Rev. Physiol.* **64,** 563–594
41. Li, C., Krishnamurthy, P. C., Penmatsa, H., Marrs, K. L., Wang, X. Q., Zaccolo, M., Jalink, K., Li, M., Nelson, D. J., Schuetz, J. D., and Naren, A. P. (2007) Spatiotemporal coupling of cAMP transporter to CFTR chloride channel function in the gut epithelia. *Cell* **131,** 940–951
42. Akanuma, S., Hosoya, K., Ito, S., Tachikawa, M., Terasaki, T., and Ohtsuki, S. (2010) Involvement of multidrug resistance-associated protein 4 in efflux transport of prostaglandin E(2) across mouse blood-brain barrier and its inhibition by intravenous administration of cephalosporins. *J. Pharmacol. Exp. Ther.* **333,** 912–919
43. Mendez, M., and LaPointe, M. C. (2005) PGE2-induced hypertrophy of cardiac myocytes involves EP4 receptor-dependent activation of p42/44 MAPK and EGFR transactivation. *Am. J. Physiol. Heart Circ. Physiol.* **288,** H2111–H2117
44. Engelhardt, S., Hein, L., Wiesmann, F., and Lohse, M. J. (1999) Progressive hypertrophy and heart failure in beta1-adrenergic receptor transgenic mice. *Proc. Natl. Acad. Sci. U. S. A.* **96,** 7059–7064
45. Gaudin, C., Ishikawa, Y., Wight, D. C., Mahdavi, V., Nadal-Ginard, B., Wagner, T. E., Vatner, D. E., and Homcy, C. J. (1995) Overexpression of Gs alpha protein in the hearts of transgenic mice. *J. Clin. Invest.* **95,** 1676–1683
46. Iwase, M., Bishop, S. P., Uechi, M., Vatner, D. E., Shannon, R. P., Kudej, R. K., Wight, D. C., Wagner, T. E., Ishikawa, Y., Homcy, C. J., and Vatner, S. F. (1996) Adverse effects of chronic endogenous sympathetic drive induced by cardiac GS alpha overexpression. *Circ. Res.* **78,** 517–524
47. Feldman, D. S., Carnes, C. A., Abraham, W. T., and Bristow, M. R. (2005) Mechanisms of disease: beta-adrenergic receptors–alterations in signal transduction and pharmacogenomics in heart failure. *Nat. Clin. Pract. Cardiovasc. Med.* **2,** 475–483
48. Bristow, M. R. (1998) Why does the myocardium fail? Insights from basic science. *Lancet* **352**(Suppl. 1), SI8–SI14
49. Cohn, J. N., Goldstein, S. O., Greenberg, B. H., Lorell, B. H., Bourge, R. C., Jaski, B. E., Gottlieb, S. O., McGrew, F., 3rd, DeMets, D. L., and White, B. G. (1998) A dose-dependent increase in mortality with vesnarinone among patients with severe heart failure. Vesnarinone trial investigators. *N. Engl. J. Med.* **339,** 1810–1816
50. Packer, M., Carver, J. R., Rodeheffer, R. J., Ivanhoe, R. J., DiBianco, R., Zeldis, S. M., Hendrix, G. H., Bommer, W. J., Elkayam, U., Kukin, M. L., Mallis, G. I., Solano, G. A., Shannon, J., Tandon, P. K., DeMets, D. L., and the PROMISE study research group. (1991) Effect of oral milrinone on mortality in severe chronic heart failure. The PROMISE Study Research Group. *N. Engl. J. Med.* **325,** 1468–1475
51. Copsel, S., Garcia, C., Diez, F., Vermeulem, M., Baldi, A., Bianciotti, L. G., Russel, F. G., Shayo, C., and Davio, C. (2011) Multidrug resistance protein 4 (MRP4/ABCC4) regulates cAMP cellular levels and controls human leukemia cell proliferation and differentiation. *J. Biol. Chem.* **286,** 6979–6988

Received for publication September 6, 2011.
Accepted for publication November 1, 2011.